JOURNAL OF COMPUTATIONAL PHYSICS 101, 71–79 (1992)

A Numerical Energy Conserving Method for the DNLS Equation

TOR FLÅ

Institute of Mathematical and Physical Sciences, University of Tromsø, N-9001 Tromsø, Norway

Received April 28, 1989; revised September 30, 1991

An implicit, numerical energy conserving method is developed for the derivative nonlinear Schrödinger (DNLS) equation for periodic boundary conditions. We find no numerical high frequency modulational instabilities in addition to the modulational instability from a linear analysis around a nonlinear state for the DNLS equation if the modulation is small and $(k_0 - a^2/2)^2 \tau < \pi$ (k_0 is the wavenumber and a the amplitude). The numerical scheme is used to follow the nonlinear behavior of the DNLS modulational instability. The numerical code is also tested by the evolution for one soliton initial data. These tests show that if the modulation is not small compared to the background wave amplitude, new nonlinear numerical instabilities are introduced.

1. INTRODUCTION

The purpose of this work is to study the stability of a numerical method designed to solve the derivative nonlinear Schrödinger (DNLS) equation for periodic boundary conditions. The DNLS equation has been used to model weakly nonlinear, dispersive, and circular polarized parallel propagating Alfvén waves [1–3]. It has also been used to model extremely short solitary waves in optical fibers [4]. The DNLS equation can be written in the form [1]

$$q_t + (|q|^2 q)_x + iq_{xx} = 0. \tag{1}$$

Here $q(x, t) \in \mathbf{C}$ is the complex amplitude and x and t are normalized space and time coordinates. Two types of exact solutions to the DNLS equation have been studied theoretically—self-modulated soliton wave packets and constant amplitude wave trains. Recent theoretical work [5, 6] have extended the DNLS model of parallel propagating Alfvén waves to include the effect of a small nonlocal term due to resonant particles [5] and also more general perturbations [6]. Numerical works on the DNLS equation have been done in [7, 8, 20, 21]. In most of these works the DNLS equation are integrated by calculating nonlinearities at spatial gridpoints and performing time steps at the respective discrete points in Fourier space by applying a FFT [9, 10]. Dawson *et al.* [21] have, however, recently discussed a fast algorithm using a gauge transformation and a modification of the Ablowitz–Ladik method [32].

Numerical instability for nonlinear evolution equations have only recently been studied in detail. A lot of study has been done of the convective equation [11–17] and lately, also, of augmented Hamiltonian systems [18] and quasilinear pseudo-parabolic equations [19]. Our work will be based on a method to study numerical modulational instability of constant amplitude wave trains, first suggested in [22] and worked out in detail in [23] for the NLS equation. Since our method will be shown essentially linearly, numerically stable (for practical choices of parameters), it gives an opportunity to study nonlinear, numerical instabilities by numerical tests.

Whitham and Fornberg [22] have developed a strategy to solve nonlinear evolution equations for periodic boundary conditions by calculating spatial operators in the discrete Fourier space and the nonlinear terms on a discrete grid in space (a pseudospectral method). The leapfrog technique is then used to step the solution forward in time at each grid point. In this paper a modification of the Whitham–Fornberg method will be used which is implicit in time. The method will be shown to have good numerical stability properties and to be energy conserving (Sections 2 and 3). Some sample runs of the nonlinear evolution of the modulational instability for an initially constant amplitude wave train and the evolution of a soliton will be shown in Section 4.

2. A NUMERICAL ENERGY CONSERVING METHOD

We will assume periodic boundary conditions in our study of a numerical scheme to solve the DNLS equation. The solutions therefore become L-periodic functions in space, i.e., $q(x + L) = q(x)$. Such periodic functions can be resolved in a Fourier series

$$q(x) = \sum_{n=-\infty}^{\infty} c_n \exp(ik_n x), \tag{2}$$

0021-9991/92 $5.00

where c_n is the Fourier coefficient given by

$$c_n = \frac{1}{L}\int_{-L/2}^{L/2} q(x)\exp(-ik_n x)\,dx, \qquad k_n = \frac{2\pi n}{L}; \quad n \in \mathbf{Z}. \tag{3}$$

However, on a computer only a finite number of Fourier modes and grid points can be used. The discrete, symmetric Fourier transform, F, becomes, when we use an odd number $(N+1)$ of grid points (x_j),

$$\hat{q}_n = \frac{1}{(N+1)}\sum_{j=-N/2}^{N/2} q_j \exp(-ik_n x_j) = (F(q_j))_n. \tag{4}$$

Here

$$x_j = \frac{L}{(N+1)}j, \qquad j \in [-N/2, N/2]$$

and

$$q_j = q(x_j).$$

(For convenience the formulas are written for the case when N is odd. However, some of the simulations are done for N even.) It can be shown that the truncated inversion formula

$$\tilde{q} = \sum_{n=-N/2}^{N/2} \hat{q}_n \exp(ik_n x) \tag{5}$$

represents $q_j = \tilde{q}(x_j) = F^{-1}(\hat{q}_n)$ exactly at the grid points. To show this, the formula

$$\sum_{n=-N/2}^{N/2} \exp(ik_n(x_j - x_{j'})) = (N+1)\,\delta_{j,j'}, \tag{6}$$

is needed. $\tilde{q}(x)$ can therefore be looked upon as an interpolation formula for $q(x)$ based on the $(N+1)$ grid points. This interpolation formula gives us the opportunity to estimate operators like, e.g., the derivative of the solution at the grid points,

$$(\tilde{q}_x)_j = \sum_{n=-N/2}^{N/2} ik_n \hat{q}_n \exp(ik_n x_j). \tag{7}$$

Linear and nonlinear evolution equations have been solved by several authors (e.g., [9, 10, 25, 26]), using the so-called spectral method which often is implemented with periodic boundary conditions and cutoffs in Fourier space to avoid numerical instabilities. The Whitham–Fornberg method [22, 24] claims to show no numerical instabilities due to aliasing. Spangler *et al.* [7] integrated the DNLS equation numerically in time in a Fourier space with a cutoff to avoid aliasing instabilities. However, the Whitham–Fornberg method does not seem to work on the DNLS equation with leapfrog time integration in the numerical experiments that I have done. An iterative, implicit modification of the Whitham–Fornberg method therefore has been developed for the DNLS equation. The solution at time step $(m+1)$ and grid point j is found by the implicit scheme

$$\begin{aligned}
\tilde{q}_j^{m+1} &= \bar{q}_j^m - \tau[2\,|\tilde{q}_j'^m|^2\,(\tilde{q}_x')_j^m + (\tilde{q}_j'^m)^2\,(\tilde{q}_x'^*)_j^m],\\
\bar{q}_j^m &= F^{-1}(\hat{q}_n^m e^{ik_n^2\tau})_j,\\
\tilde{q}_j'^m &= \tfrac{1}{2}(\tilde{q}_j^{m+1} + \bar{q}_j^m),\\
(\tilde{q}_x')_j^m &= \tfrac{1}{2}F^{-1}(ik_n(\hat{q}_n^{m+1} + \hat{q}_n^m e^{ik_n^2\tau})).
\end{aligned} \tag{8}$$

Here τ is the time step and * denotes complex conjugation. Note that the linear terms are integrated exactly while the nonlinear terms are consistent with Eq. (1) when $\tau \to 0$.

The DNLS equation can be shown to have an infinite hierarchy of conservation equations [27]. For vanishing and periodic boundary conditions these conservation equations define conserved quantities in time. The first two conserved quantities for periodic boundary conditions are the average complex amplitude (q_{av}) and total energy content (E_p) in one period

$$q_{\mathrm{av}} = \frac{1}{L}\int_{-L/2}^{L/2} q\,dx, \tag{9}$$

$$E_p = \int_{-L/2}^{L/2} |q|^2\,dx. \tag{10}$$

Both these conservation laws are reproduced by our numerical scheme Eq. (8) and Eq. (6) as

$$\tilde{q}_{\mathrm{av}} = \frac{1}{(N+1)}\sum_{j=-N/2}^{N/2} \tilde{q}_j^{m+1} = \frac{1}{(N+1)}\sum_{j=-N/2}^{N/2} \tilde{q}_j^m, \tag{11}$$

$$\tilde{E}_p = \sum_{j=-N/2}^{N/2} |\tilde{q}_j^{m+1}|^2\,\Delta x = \sum_{j=-N/2}^{N/2} |\tilde{q}_j^m|^2\,\Delta x, \tag{12}$$

$$\Delta x = L/(N+1).$$

The conservation of the average complex amplitude is found by simply looking at the time evolution of the zeroth discrete Fourier transform, $\hat{q}_o$, from (8). The numerical conservation law for the energy, $\tilde{E}_p$, is obtained by multiplying (8) with $\tilde{q}_j'^{m*}$ and the complex conjugate of (8) with $\tilde{q}_j'^m$, summing these two expressions and then summing the results over the space grid index j.

Before we leave the numerical energy conserving method, we will dwell on its ability to reproduce the dispersion relation for the DNLS equation [1] for a constant amplitude

wave train with frequency ω, wave number k_o, and amplitude a,

$$\omega = k_o(a^2 - k_o). \tag{13}$$

We represent the discrete version of the wave train as (note that in the following, we will use ω to represent the frequency both in the continuous and discrete case)

$$\tilde{q}_j^m = a \exp(i(k_o x_j - \omega m\tau)),$$

and find the numerical dispersion relation

$$\sin((\omega + k_o^2)\tau) = k_o a^2 \tau[\tfrac{1}{2}(1 + \cos((\omega + k_o^2)\tau))]^2 \tag{14}$$

which for $k_o a^2 \tau \ll 1$ can be written

$$\omega \approx k_o(a^2[1 - \tfrac{1}{2}(k_o a^2 \tau)^2] - k_o). \tag{15}$$

From this expression we deduce that the relative truncation error of the dispersion relation is $O(\frac{1}{2}(k_o a^2\tau)^2)$. An estimate of the relative truncation error for the wave train based on (15) is, after a time, $t = m\tau$,

$$\Delta = \left|\frac{\Delta q}{q}\right| \approx \frac{1}{2} t(k_o a^2)^3 \tau^2. \tag{16}$$

The numerical scheme therefore reproduces the nonlinear dispersion relation for a constant amplitude wave train well for time steps

$$\tau \ll \sqrt{2}/k_o a^2. \tag{17}$$

Even if we take care to use parameters corresponding to small truncation errors, we can only expect the constant amplitude wave train to be well reproduced for total times $t = m\tau$, such that

$$t \ll \frac{2}{(k_o a_o^2)^3 \tau^2}. \tag{18}$$

However, the nonlinear wave train may be subject to growth due to numerical, modulational instabilities. These numerical instabilities and the restrictions they put on the parameters to reproduce the DNLS results are discussed in the next section.

3. NUMERICAL STABILITY OF THE ENERGY CONSERVING METHOD

The numerical modulational instability of a constant amplitude wave train was investigated in [23] for the split-step method to integrate the nonlinear Schrödinger (NLS) equation in time both for a finite difference and spectral method in space. We intend in this section to follow up this work on the energy conserving method for the DNLS equation.

3.1. *Modulational Instability for the DNLS Equation for Periodic Boundary Conditions*

First we will briefly study the modulational instability for the DNLS equation for periodic boundary conditions. This represents the theoretical state to which our investigation of numerical instability should be compared. The modulation of the constant amplitude wave train is expressed by

$$q = \hat{q}(1 + \varepsilon(x, t)), \tag{19}$$

$$\hat{q} = a \exp(i(k_o x - \omega t)). \tag{20}$$

Here q, $\hat{q}$, and ε ($\in \mathbf{C}$) are L-periodic functions on the interval $[-\frac{1}{2}L, \frac{1}{2}L]$, and $|\varepsilon|^2 \ll 1$. If one puts (19) into the DNLS equation, the following approximate equation for the modulation is obtained

$$\varepsilon_t + i\varepsilon_{xx} + ik_o a^2(\varepsilon + \varepsilon^*) + 2(a^2 - k_o)\,\varepsilon_x + a^2\varepsilon_x^* = 0. \tag{21}$$

The perturbation on the amplitude, $\varepsilon(x, t)$, may be expanded in a Fourier series

$$\varepsilon(x, t) = \sum_{n=-\infty}^{\infty} \hat{\varepsilon}_n(t) \exp(i\mu_n x),$$

where the modulational wavenumber $\mu_n = 2\pi n/L$, $n \in \mathbf{Z}$. From (21) $\hat{\varepsilon}_o(t)$ will be found to be a constant which without loss of generality can be set to zero. From (21) we can deduce

$$\frac{d}{dt}\begin{pmatrix} \hat{\varepsilon}_n \\ \hat{\varepsilon}_{-n}^* \end{pmatrix} = C_n \begin{pmatrix} \hat{\varepsilon}_n \\ \hat{\varepsilon}_{-n}^* \end{pmatrix}, \tag{22}$$

$$C_n = i\begin{pmatrix} k_0 a^2 + 2(a^2 - k_0)\mu_n - \mu_n^2 & a^2(k_0 + \mu_n) \\ -a^2(k_0 - \mu_n) & -k_0 a^2 + 2(a^2 - k_0)\mu_n + \mu_n^2 \end{pmatrix}.$$

If one assumes

$$\begin{pmatrix} \hat{\varepsilon}_n(t) \\ \hat{\varepsilon}_{-n}^*(t) \end{pmatrix} = \begin{pmatrix} \hat{\varepsilon}_n(0) \\ \hat{\varepsilon}_{-n}^*(0) \end{pmatrix} \exp(\Lambda_n t),$$

we obtain

$$\Lambda_n = i2(a^2 - k_0)\,\mu_n \pm |\mu_n|\,((2k_0 - a^2)\,a^2 - \mu_n^2)^{1/2}. \tag{23}$$

Equation (23) shows that the constant amplitude wave train is unstable for $k_0 > a^2/2$ and marginally stable for

$k_0 < a^2/2$ (cf. [1]). The initial disturbance will, if both eigenmodes are present, grow exponentially in time for $0 < \mu_n^2 < a^2(2k_0 - a^2)$.

3.2. *Modulational Instability for the Energy Conserving Scheme*

It is intuitively expected that a numerical scheme which conserves energy also should show good properties with respect to numerical stability. Let us therefore investigate this conjecture for small modulations on a constant amplitude wave train. The modulation of the constant amplitude wave train is written as

$$\begin{aligned} \tilde{q}_j^m &= (1+\varepsilon_j^m)a\exp(i(k_0 x_j - \omega m\tau), \\ \varepsilon_j^m &= \sum_{n=-N/2}^{N/2} \hat{\varepsilon}_n^m \exp(i\mu_n x_j). \end{aligned} \tag{24}$$

The linearized equation for ε_j^m is found from Eq. (8),

$$\begin{aligned} & e^{-i\omega\tau}\left(1+\tau a^2 s_0\left(ik_0+\frac{\partial}{\partial x}\right)\right)\varepsilon_j^{m+1} \\ & \quad +\frac{1}{2}\tau a^2 s_1 e^{i\omega\tau}\left(ik_0+\frac{\partial}{\partial x}\right)\varepsilon_j^{m+1*} \\ & = e^{-i\omega\tau}\varepsilon_j^m + \not{\varepsilon}_j^m \\ & \quad -\tau a^2\left(-ik_0 s\varepsilon_j^m + s_0\left(ik_0+\frac{\partial}{\partial x}\right)\tilde{\varepsilon}_j^m\right) \\ & \quad -\frac{\tau a^2}{2}s_1\left(ik_0+\frac{\partial}{\partial x}\right)\tilde{\varepsilon}_j^{m*}, \end{aligned} \tag{25}$$

$$\begin{aligned} \not{\varepsilon}_j^m &= \sum_{n=-N/2}^{N/2} \hat{\varepsilon}_j^m e^{i\mu_n x_j}(e^{i(\mu_n+k_0)^2\tau} - e^{ik_0^2\tau}), \\ \tilde{\varepsilon}_j^m &= \sum_{n=-N/2}^{N/2} \hat{\varepsilon}_n^m e^{i((\mu_n+k_0)^2\tau + \mu_n x_j)}, \\ s &= \tfrac{1}{4}[1+\cos((\omega+k_0^2)\tau)](e^{-i\omega\tau}+e^{ik_0^2\tau}), \\ s_0 &= \tfrac{1}{2}(1+\cos((\omega+k_0^2)\tau)), \\ s_1 &= \tfrac{1}{4}(e^{-i\omega\tau}+e^{ik_0^2\tau})^2. \end{aligned}$$

Here the operator $\partial/\partial x$ is defined in Eq. (7). The time development for the Fourier coefficients of the modulation is given by

$$A_n\begin{pmatrix}\hat{\varepsilon}_n^{m+1}\\ \hat{\varepsilon}_{-n}^{m+1*}\end{pmatrix} = G_n\begin{pmatrix}\hat{\varepsilon}_n^m\\ \hat{\varepsilon}_{-n}^{m*}\end{pmatrix},$$

$$A_n(\tau) = \begin{pmatrix} 1+i\tau a^2 s_0(k_0+\mu_n) & \frac{i}{2}\tau a^2 s_1(k_0+\mu_n)\,e^{i2\omega\tau} \\ \frac{i}{2}\tau a^2 s_1^*(-k_0+\mu_n)\,e^{-i2\omega\tau} & 1+i\tau a^2 s_0(-k_0+\mu_n)\end{pmatrix},$$

$$G_n(\tau) = \begin{pmatrix} a_1 & b_1 \\ c_1 & d_1\end{pmatrix}, \tag{26}$$

$$\begin{aligned} a_1 &= [1+(e^{i(\mu_n+k_0)^2\tau} - e^{ik_0^2\tau})\,e^{i\omega\tau} \\ &\quad - i\tau a^2 e^{i\omega\tau}(-k_0 s + s_0(k_0+\mu_n)\,e^{i(\mu_n+k_0)^2\tau})], \\ b_1 &= -\frac{i}{2}\tau a^2 s_1(k_0+\mu_n)\cdot e^{i(-(\mu_n-k_0)^2+\omega)\tau}, \\ c_1 &= -\frac{i}{2}\tau a^2 s_1^*(-k_0+\mu_n)\,e^{i((\mu_n+k_0)^2-\omega)\tau}, \\ d_1 &= [1+(e^{-i(\mu_n-k)^2\tau} - e^{ik_0^2\tau})\,e^{-i\omega\tau} \\ &\quad - i\tau a^2 e^{-i\omega\tau}(k_0 s^* + s_0(-k_0+\mu_n)\cdot e^{-i(\mu_n-k_0)^2\tau})]. \end{aligned}$$

Let us first make sure that the time developments converge to the same one that we obtained in Eq. (22)–(23) when $\tau \to 0$. The time evolution of (26) at the mth time step

$$\begin{pmatrix}\hat{\varepsilon}_n^m\\ \hat{\varepsilon}_{-n}^{m*}\end{pmatrix} = \begin{pmatrix}\hat{\varepsilon}_n^0\\ \hat{\varepsilon}_{-n}^{0*}\end{pmatrix}(\kappa_n(\tau))^m = \begin{pmatrix}\hat{\varepsilon}_n^0\\ \hat{\varepsilon}_{-n}^{0*}\end{pmatrix} e^{m\Lambda_n(\tau)\tau}. \tag{27}$$

Here $\kappa_n(\tau) = e^{\Lambda_n(\tau)\tau}$ is the factor which gives the change in the complex amplitude of the Fourier coefficients from one time step to another. $\Lambda_n(\tau)$ is just a different way to express this coefficient which is closer to the eigenvalue parameter (cf. (23)) in the continuous case. Formally κ_n are found as eigenvalues of $A_n^{-1}G_n$,

$$\det(-\kappa_n I + A_n^{-1}G_n) = 0. \tag{28}$$

We find growing solutions if $|\kappa_n| > 1$ or $\mathrm{Re}(\Lambda_n) > 0$ and from this, one should be able to find the exact parameter regimes for stable/unstable nearly constant amplitude wave trains. However, even if the solution of κ_n is formally trivial the discussion of the exact parameter regime for stability seems to be exceedingly complicated in this case. If we make an expansion of Λ_n, A_n, and G_n for small τ we obtain

$$\begin{aligned} \Lambda_n(\tau) &= \Lambda_{n0} + \Lambda_{n1}\tau + \cdots, \\ A_n(\tau) &= A_n(0) + \frac{dA_n}{d\tau}(0)\tau + \cdots, \\ G_n(\tau) &= G_n(0) + \frac{dG_n}{d\tau}(0)\tau + \cdots, \\ A_n(0) &= G_n(0) = I. \end{aligned} \tag{29}$$

To lowest order in τ we find the eigenvalue Λ_{n0} given by

$$\det\left(-\Lambda_{n0}I + \left(\frac{dG_n(0)}{d\tau} - \frac{dA_n(0)}{d\tau}\right)\right) = 0.$$

After some calculations we obtain exactly the same expression for Λ_{n0} as in (23).

Earlier, we have concluded that the numerical dispersion

relation for a constant amplitude wave train is only close to the DNLS dispersion relation if $(\omega + k_0^2)\tau \approx k_0 a^2 \tau \ll 1$. Since (28) seems to be difficult to discuss otherwise (and this restriction is the only way to reproduce the DNLS behavior), let us expand (28) with $k_0 a^2 \tau$ as a small parameter. It can then be shown that

$$A_n^{-1} G_n \approx (\det A_n)^{-1} e^{i2\mu_n k_0 \tau} \cdot \begin{pmatrix} a_2 & b_2 \\ c_2 & d_2 \end{pmatrix}, \tag{30}$$

$$a_2 = e^{i\mu_n^2 \tau}(\beta_n - ik_0 a^2 \tau),$$

$$b_2 = -\frac{i}{2}\tau a^2 s_1 (\mu_n + k_0)(2 - ik_0 a^2 \tau - k_0 a^4 \mu_n^2 \tau^2)\, e^{-i\mu_n^2 \tau},$$

$$c_2 = -\frac{i}{2}\tau a^2 s_1^* (\mu_n - k_0)(2 + ik_0 a^2 \tau + k_0 a^4 \mu_n \tau^2)\, e^{i\mu_n^2 \tau},$$

$$d_2 = e^{-i\mu_n^2 \tau}(\beta_n + ik_0 a^4 \tau),$$

$$\beta_n = 1 + \mu_n^2 \tau^2 a^4 - \frac{\tau^2 a^4}{4}(\mu_n^2 - k_0^2),$$

$$\det A_n \approx 1 + i2\tau a^2 \mu_n - \tau^2 a^4 (\mu_n^2 - k_0^2)\, \tfrac{3}{4}.$$

In this approximation we can reduce (28) to

$$\begin{aligned}(-\alpha_n + \beta_n \cos(\mu_n^2 \tau) + k_0 a^2 \tau \sin(\mu_n^2 \tau))^2 \\ + (\beta_n \sin(\mu_n^2 \tau) - k_0 a^2 \tau \cos(\mu_n^2 \tau))^2 \\ + \tau^2 a^4 (\mu_n^2 - k_0^2) \approx 0.\end{aligned} \tag{31}$$

$$\kappa_n = e^{i2\mu_n k_0 \tau} \frac{\alpha_n}{\det A_n}. \tag{32}$$

The solution is obtained as

$$\begin{aligned}\alpha_n \approx \beta_n \cos(\mu_n^2 \tau) + k_0 a^2 \tau \sin(\mu_n^2 \tau) \\ \pm i((\beta_n \sin(\mu_n^2 \tau) - k_0 a^2 \tau \cos(\mu_n^2 \tau))^2 \\ + \tau^2 a^4 (\mu_n^2 - k_0^2))^{1/2}.\end{aligned} \tag{33}$$

The absolute value of the expansion coefficient, $|\kappa_n|$, can then be found if the term inside the squareroot in Eq. (33) is positive (e.g., outside the region of growth for DNLS),

$$\begin{aligned}|\kappa_n|^2 \approx (d_n + \tfrac{1}{2}(k_0 a^2 \tau)^2)/(d_n + \tfrac{3}{2}(k_0 a^2 \tau)^2), \\ d_n = 1 + \tfrac{5}{2}\mu_n^2 a^4 \tau^2 + \tfrac{9}{16}(\mu_n^2 a^4 \tau^2)^2.\end{aligned} \tag{34}$$

Equation (34) shows that the constant wave train is close to marginally stable ($|\kappa_n| \approx 1$) if $(k_0 a^2 \tau) \ll 1$ as it should in the parameter regime where no modulational instability is expected for the DNLS equation. In addition the numerical energy conserving method is stable in this regime since $|\kappa_n| \lesssim 1$. It must, however, be cautioned that this analysis does not say anything about numerical stability when $k_0 a^2 \tau$ approaches one and that we must indeed expect large numerical errors if $\tau \geqslant 1/(k_0 a^2)$.

Let us now try to find the expansion factor, κ_n, to $O(\tau^2)$ in a situation with growth for the DNLS solution $k_0 > a^2/2$ and $0 < \mu_n^2 < (2k_0 - a^2)\, a^2$. If we assume that $\mu_n^2 \tau \ll 1$, $k_0 a^2 \tau \ll 1$, and $\mu_n a^2 \tau \ll 1$, we find

$$\begin{aligned}\kappa_n = e^{\Lambda_n \tau} = e^{(\Lambda_{n0} + \Lambda_{n1}\tau)\tau} \approx e^{\Lambda_{n0}\tau}(1 + \Lambda_{n1}\tau^2), \\ \Lambda_{n1} = \tfrac{1}{2}\mu_n^4 - \mu_n^2 (k_0 + a^2)\, a^2 - \tfrac{1}{2}(k_0 a^2)^2.\end{aligned} \tag{35}$$

We observe that, both for the situations with growing and nongrowing solutions, the numerical scheme gives rise to an error of $O(\tau^2)$ compared to the theoretical predictions (for each timestep).

For $\mu_n^2 \tau \to 0_+$ we expect to regain the modulational instability for the DNLS equation for $k_0 > a^2/2$. In addition there is the possibility that additional strong, high frequency modulational instabilities of pure numerical origin, may appear as bands of growth around $\mu_n^2 \tau = k\pi$, $k = +1, +2, \ldots$ [23]. A sufficient condition for stability is that

$$(\beta_n \sin(\mu_n^2 \tau) - k_0 a^2 \tau \cos(\mu_n^2 \tau))^2 + \tau^2 a^4 (\mu_n^2 - k_0^2) \geqslant 0. \tag{36}$$

If $k_0 a^2 \tau$, $a^4 \tau \ll 1$, we can only have equality for $(\mu_n^2 \tau - k\pi) \ll 1$, $k \geqslant 1$. The solution for the expression (36) equal to zero in this case is approximately

$$\begin{aligned}\mu_n^2 \tau \approx k\pi + [(2k_0 a^2 - a^4)\tau \pm ((2k_0 a^2 - a^4)^2 \tau^2 \\ - 4a^4 k\pi\tau)^{1/2}]/2, \qquad k \geqslant 0.\end{aligned} \tag{37}$$

We have a modulational stable wave train if

$$\left| k_0 - \frac{a^2}{2} \right| < \sqrt{k\pi/\tau}, \qquad k > 0 \tag{38}$$

or

$$k_0 < \frac{a^2}{2}, \qquad k = 0. \tag{39}$$

Equation (39) is recognized as the stability criterion for a constant amplitude wave train solution of the DNLS equation. However, additional parameter regions of pure numerical origin will be obtained from (38). Of course the numerical code will be stable if $\mu_{N/2}^2 \tau < \pi$ which is the high frequency modulational stability criterion obtained in [22, 23]. What is extraordinary for the energy-conserving scheme is that *no numerical high frequency modulation*

instabilities are observed even if $\mu_{N/2}^2\tau > \pi$, as long as parameters are chosen such that

$$\left(k_0 - \frac{a^2}{2}\right)^2 \tau < \pi. \tag{40}$$

But we are already restricted to parameters such that $k_0 a^2 \tau \ll 1$. In general one will also choose $\mu_{N/2} > k_0$ to resolve the wave train. This means that the severe restriction on the time step $\tau < \pi^{-1}\,\Delta x^2$ as a function of spatial resolution, which is reported in [22, 23] is greatly alleviated for small modulations if, in addition, the amplitude is not too large ($\tau < 4\pi/a^4$). Instead of a modulational stability criterion which depends on the spatial resolution, we have obtained one which depends solely on the amplitude (a) and on the local wavenumber (k_0). Strictly, our analysis is only relevant for small amplitude modulations on a constant amplitude wave train. However, in the next section we will show sample runs of the nonlinear evolution of a self-modulated soliton wave packet and modulated wave trains.

4. NUMERICAL TESTS

The motivation for this section is to document through numerical tests that it is indeed possible to run this code for the DNLS equation even for timesteps $\tau > \pi^{-1}\,\Delta x^2$ when the nonlinear evolution is not too far from the constant amplitude case. We will also discuss the possibility of nonlinear numerical instabilities. Dawson *et al.* [21] have recently discussed a fast code for the DNLS equation using a gauge transformation from the AKNS inverse scattering problem [28] to the Kaup–Newell inverse scattering problem [27]. However, numerical instabilities were not discussed and if the code is as fast for large amplitude and deep modulations has not been studied. Other workers have developed numerical codes for the DNLS equation [7, 20], but none of these workers, as far as I know, have discussed nonlinear numerical instabilities.

The relative truncation error for a constant amplitude wave train will by inspection be found to be extremely small compared to what we can calculate from numerical simulations when the wave train is unstable, $k_0 > a^2/2$. However, we can use our estimate of the deviation from the theoretical DNLS expansion factor (35) (in the stable case these deviations give rise to very small errors in the amplitude if the modulation amplitude is small) to argue for an estimate for the nonlinear relative error. To leading order the error in the expansion factor

$$|\Delta\kappa_n| \approx |\Lambda_{n1}|\,\tau^2 \cdot |\kappa_n|. \tag{41}$$

Here Λ_{n1} is given in Eq. (35).

The expansion factor will in reality be following a recurrence cycle, T_{rec} (if the solution is recurrent), and we intuitively assume (cf. Eq. (40)) that the error in the expansion factor and the generated error in the solution itself will follow a similar recurrence cycle. From Eq. (40), we can argue that the maximal relative error during one cycle is

$$\Delta = \left|\frac{\Delta q}{q}\right| \approx \alpha \frac{a_1}{a} \cdot \Lambda_{n1}\tau T_{\text{rec}}. \tag{42}$$

(If we use the natural scaling $k_0 = Xa^2$ and $\mu_n = Ya^2$, we find that $\Delta \sim a^4\tau$.) Here a_1 is the maximal amplitude of the modulation and α is some numerical factor which takes care of the scaling of other nonlinear effects. For small initial modulations ($\varepsilon \ll 1$) an estimate of the maximal amplitude can be given from my theoretical and numerical investigation in [31]

$$a_1^2 \approx \frac{2\Lambda_{n0}^2}{\mu_n^2 k_0}, \tag{43}$$

while the recurrence time is estimated as

$$T_{\text{rec}} \approx \frac{1}{\Lambda_{n0}} \ln\left(16\,\frac{a_1^2}{a_{\min}^2}\right). \tag{44}$$

Here Λ_{n0} is given as the real part of Eq. (23); $a_{\min}$ is the minimal amplitude of the modulations which we can estimate as $a_{\min} \sim \varepsilon a$, where ε is the relative modulation amplitude.

One can now suggest the following nonlinear numerical instability mechanism. Under stable conditions the numerical error in the recurrent amplitude will be locked to the recurrence cycle of the unstable mode. However, the numerical deviation from the exact recurrent mode will presumably be able to excite new recurrent modes with $a_{\min 1} \sim a\Delta$ if the new recurrence time

$$T_{\text{rec}\,1} \leqslant T_{\text{rec}}. \tag{45}$$

Note that the maximal amplitude (cf. (43)) in these modulations will be of the same magnitude or larger than the original amplitudes. The theoretical DNLS solution will therefore be destroyed. If one further makes the assumption that the new modulation has approximately the same modulation wavenumber as the original, one finds from Eqs. (44), (45) the simple stability criterion

$$\Delta < a_{\min}. \tag{46}$$

If instead one assumes that it is the fastest growing mode which is excited, one obtains the order of magnitude estimate

$$\Delta < (a_{\min})^{\kappa}, \qquad \kappa = \frac{\Lambda_{n0f}}{\Lambda_{n0}}. \tag{47}$$

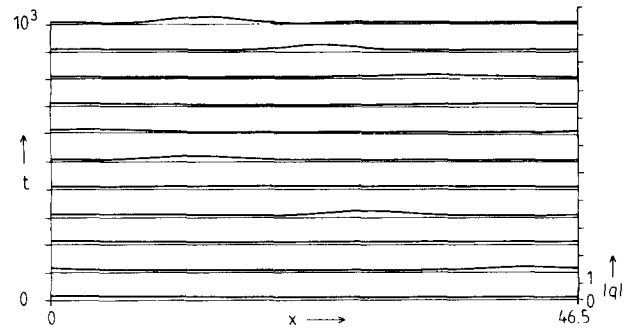

FIG. 1. These figures display spatial time series of the numerical solution of the DNLS equation for two different numerical time steps. The normalized amplitude $a = 0.15$, the normalized periodic window has a length $L = 46.54$ and is divided into $N = 256$ points ($\Delta x \approx 0.18$), the wavenumber $k_0 = 1.215$, the modulational wavenumber $k_1 = 0.135$, and the relative modulational amplitude $\varepsilon = 5 \times 10^{-2}$. Here the initial data are chosen as $q(x) = ae^{ik_0 x}(1 + \varepsilon(e^{ik_1 x} + e^{-ik_1 x}))$. The numerical solution of the DNLS equation when the numerical time step is $\tau = 0.2$ and the time step between each solution displayed is $\Delta t = 100$.

Here $\Lambda_{n0f} = (2k_0 - a^2)\, a^2/2$ is the fastest growing mode's growth rate. (The numerical scheme that we are using is implicit and is begun by putting $\tilde{q}_j^{m+1} \approx \tilde{q}_j^m$ on the left side of Eq. (8) and by finding a new estimate of $\tilde{q}_j^{m+1}$. Only two to four iterations usually are used because the numerical errors, as we have seen, are of $O(\tau^2)$ anyway. In addition we have introduced a cut in Fourier space when calculating the nonlinear terms to avoid aliasing instabilities, although this does not seem to be necessary in many of the runs.)

In Figs. 1a, b and Figs. 2a, b, we have presented numerical results where the classical upper limit on the numerical time step to avoid high frequency instabilities typically would be $\tau_c = (1/\pi)\, \Delta x^2 \approx 1.06 \times 10^{-2}$ [22]. In Fig. 1 we are running a case with $\mu_n = 0.135$, $k_0 = 1.215$, $\varepsilon = 5 \times 10^{-2}$, and $a = 0.15$. This corresponds to $\Delta \approx 8.8 \cdot 10^{-3}\tau$ (if $\alpha \approx \frac{1}{25}$) and the nonlinear stability criterion $\tau < \{^{5.7}_{0.1}$. (The smallest value corresponds to the fastest growing mode.) When $\tau = 0.2$, we find $\Delta \approx 1.8 \times 10^{-3}$, which can be compared with the numerically calculated relative error in the first sideband, $\Delta_{\text{est}} \approx 1.8 \times 10^{-3}$. For $\tau = 0.5$ the numerical solution becomes unstable when the relative error becomes large enough.

In Figs. 2a, b we display a case with $\mu_n = 0.675$, $k_0 = 1.215$, $\varepsilon = 5 \times 10^{-2}$, and $a = 0.5$. Now $\Delta \approx 0.136\tau$ and the nonlinear stability criterion is $\tau < \{^{0.4}_{7.5 \times 10^{-2}}$. For Fig. 2a, $\tau = 2 \times 10^{-3}$, $\Delta \approx 2.7 \times 10^{-4}$, while $\Delta_{\text{est}} \approx 1.2 \times 10^{-4}$. The solution in this case is much more deeply modulated and further from a constant amplitude wave train. In Fig. 2b we use $\tau = 5 \times 10^{-2}$; i.e., we are close to the estimated unstable regime. Here $\Delta = 6.8 \times 10^{-3}$ and $\Delta_{\text{est}} \approx 4.1 \times 10^{-3}$. The wave train survives one recurrence period before it becomes unstable near the second maximum. (The program usually obtains overflow condition when the errors can be seen with the eye. Therefore the unstable solution is not particularly spectacular.)

Finally, we will present a numerical solution which is far from a constant amplitude wave train. Here we have taken an anomalous soliton with velocity $v = 1.5$, width $\delta = \frac{2}{3}$ and a maximum amplitude, $a_m \approx 2.7$ (cf. [29]). Notice that when $t = 9$, the soliton shape fits exactly with the initial one and the position corresponds to what we can predict on a periodic grid from the given soliton velocity. The spatial grid step $\Delta x \approx 8.9 \times 10^{-2}$ corresponds to $\tau_c \approx 2.8 \times 10^{-3}$. The time step used in this case is $\tau = 2.5 \times 10^{-4}$, i.e., $\tau < \tau_c$. However, for $\tau \gtrsim 10^{-3}$ the solution becomes numerical unstable.

The local wavelength and frequency of a DNLS soliton is [29]

$$k = k_0 + \tfrac{3}{4}a^2, \qquad v = v_0 + \tfrac{3}{4}va^2, \tag{48}$$

which corresponds to a local phase velocity $v_{pk} = v/k$. Here k_0 and v_0 is the background wavenumber and frequency. If

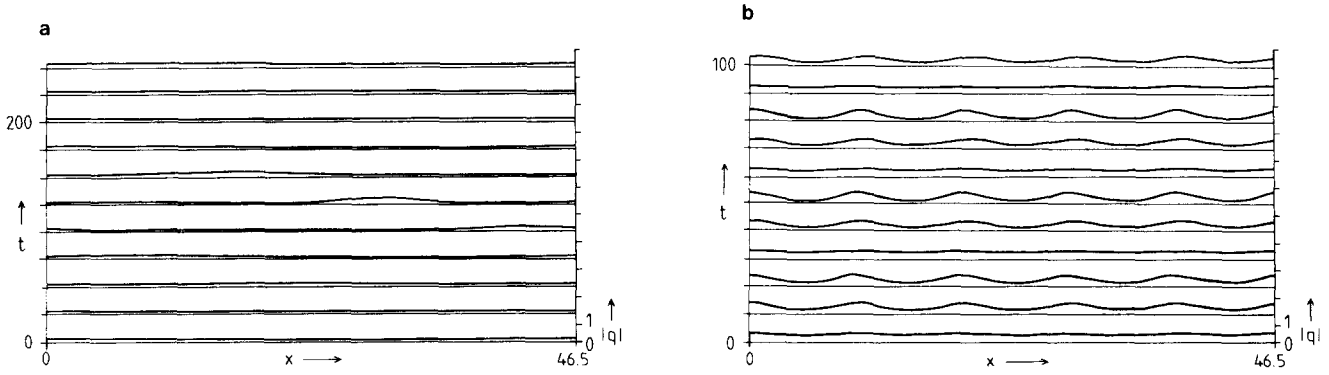

FIG. 2. This figure also displays spatial time series of the numerical solution of the DNLS equation. In this case the normalized amplitude $a = 0.5$, the normalized periodic window has a length $L = 46.54$ and is divided into $N = 256$ points, the wavenumber $k_0 = 1.215$, the modulational wavenumber $k_1 = 0.675$, and the relative modulational amplitude is $\varepsilon = 5 \times 10^{-2}$. (a) The basic numerical integration time step is $\tau = 2 \times 10^{-3}$ and the time step between each time series is $\Delta t = 10$. (b) The basic numerical integration time is $\tau = 5 \times 10^{-2}$ and the time step between each time series is $\Delta t = 5$.

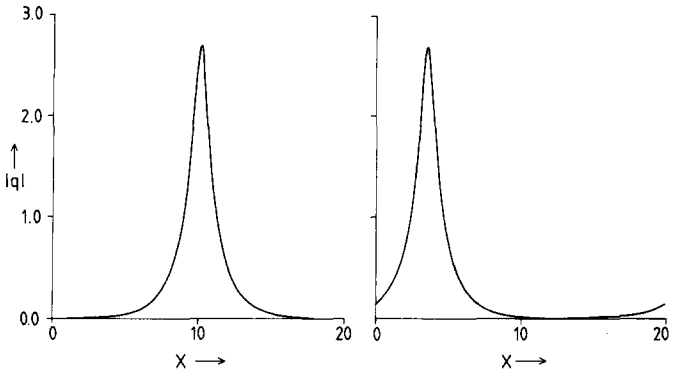

FIG. 3. Snapshots of the development of an anomalous soliton at the normalized time $t=0$ and $t=9$. The soliton parameters (cf. our work [29]) are $(\mu_0, \gamma_0)=(0.375, 0.375)$ corresponding to a background wavenumber $|k_0|=0.75$ and soliton velocity $v=1.5$. The periodic window has a length $L=20$ divided into 225 points ($\Delta x \approx 8.89\times 10^{-2}$). The basic numerical integration timestep is $\tau=2.5\times 10^{-4}$.

the velocity is not close to zero and the amplitude is large enough, we get $v_{pn}\approx v$. The characteristic timescale for the soliton is now

$$t_c=\frac{2\delta}{v_{ph}}\approx\frac{2\delta}{v}. \tag{49}$$

The relative error is assumed to accumulate and scale as

$$\Delta\approx k_0^2\tau t. \tag{50}$$

(k_0^2 is put there to obtain a^4 scaling also here.) However, in analogy with the recurrent modulations, we investigate if the soliton can adjust to the numerically accumulated error during the characteristic time scale

$$\Delta_c\approx k_0^2\tau t_c. \tag{51}$$

The fastest growing mode for the local wavenumber $k\approx\frac{1}{4}a^2$ will correspond to a growth rate and a modulation wavenumber which scale as $\Delta_{0f}=\mu_{nf}^2\sim a^4/4$. These estimates give a recurrence time

$$T_{\text{recs}}=\frac{4}{\gamma a^4}\ln\left(\frac{\frac{32}{3}\gamma}{\Delta_c^2}\right), \tag{52}$$

where γ is some numerical factor.

We conjecture in analogy with the recurrent modulations that the soliton become numerically unstable when the recurrence time for the fastest growing mode is less than the soliton's characteristic time

$$T_{\text{recs}}\leqslant t_c. \tag{53}$$

When we formulate this as a criterion for Δ and τ, we obtain

$$\begin{aligned}\Delta_c &\geqslant 4\sqrt{\frac{2}{3}}\gamma\cdot e^{-\gamma(a^4/4)\cdot(\delta/v)}\\ \tau &\geqslant 2\sqrt{\frac{2}{3}}\gamma\cdot\frac{\delta}{k_0^2 v}\cdot e^{-\gamma(a^4/4)\cdot(\delta/v)};\end{aligned} \tag{54}$$

if we take $\gamma\approx 1.5$ the numerically calculated instability criterion are approximately reproduced.

Note that, both for solitons and modulated wave trains, we obtain stability criterions which depend strongly on amplitude. This is probably the reason for the numerical problems in following unstable wavetrains near $k_0>a^2/2$ and that nobody so far has reported soliton collisions.

I suggest that the nonlinear numerical instability mechanism which have been reported here will be of the same type for any method with an error for each time step of some order in τ (except that some methods may also have high frequency instabilities). The way out seems after this remark pretty obvious. One should make Δ of higher order in τ. This can only be done by using a higher order method with no high frequency instabilities (e.g., T. Hada has told me that he is using a fourth-order, absolutely stable Runge–Kutta-type method.)

5. CONCLUSIONS

Our conclusion is that it is possible to run near constant amplitude wave trains with the energy conserving method even if $\tau\gg\tau_c=\tau^{-1}\Delta x^2$—i.e., no high frequency modulational instabilities occur. However, the relative error of deeply modulated recurrent wavetrains scales as $\Delta\sim a^4\tau$. This deviation from the theoretical recurrent mode may excite new modulational unstable modes which we conjecture will give rise to a nonlinear numerical instability if Δ is such that the recurrence time of the new modes is less than the recurrence time of the original one. We suggest that methods with a Δ which is higher order in τ and with no high frequency numerical instabilities should be searched for to avoid this nonlinear instability.

ACKNOWLEDGMENT

The numerical solutions were performed on the Norwegian Cray X/MP computer with financial support from the Norwegian Research Council (NAVF).

REFERENCES

1. E. Mjølhus, *J. Plasma Phys.* **16**, 321 (1976).
2. E. Mjølhus, *J. Plasma Phys.* **19**, 437 (1978).
3. K. Mio, T. Ogino, and K. Minami, *J. Phys. Soc. Jpn* **41**, 265 (1976).
4. P. K. Shukla and J. J. Rasmussen, *Opt. Lett.* **11**, 171 (1986).

5. E. Mjølhus and J. Wyller, *Phys. Scripta* **33**, 442 (1986).
6. J. Wyller and E. Mjølhus, *Phys. D* **13**, 234 (1984).
7. S. R. Spangler, J. P. Sheerin, and G. L. Payne, *Phys. Fluids* **28**, 104 (1985).
8. S. R. Spangler, *Ap. J.* **299**, 122 (1985).
9. D. G. Fox and S. A. Orzag, *J. Comput. Phys.* **11**, 612 (1973).
10. D. Gottlieb and S. A. Orzag, *Numerical Analysis of Spectral Methods: Theory and Applications* (SIAM, Philadelphia, 1977).
11. N. A. Phillips, "An example of non-linear computational instability," *The Atmosphere and the Sea in Motion*, edited by B. Bolin (Rockefeller Institute, New York, 1954), p. 510.
12. R. D. Richtmyer and K. W. Morton, *Difference Methods for Initial Value Problems*, 2nd ed. (Interscience, New York, 1967).
13. B. Fornberg, *Math. Comput.* **27**, 45 (1973).
14. W. L. Briggs, A. C. Newell, and T. Sarie, *J. Comput. Phys.* **51**, 83 (1983).
15. D. M. Sloan and A. R. Mitchell, *J. Comput. Phys.* **67**, 372 (1986).
16. F. Vadillo and J. M. Sanz-Serna, *J. Comput. Phys.* **66**, 225 (1986).
17. A. Cloot and B. M. Herbst, *J. Comput. Phys.* **75**, 31 (1988).
18. H. M. Hsia and Y. N. Jeng, *J. Comput. Phys.* **68**, 251 (1987).
19. A. Quarteroni, *SIAM J. Numer. Anal.* **24**, 323 (1987).
20. S. Gosh and K. Papadopoulos, *Phys. Fluids* **30**, 1371 (1987).
21. S. P. Dawson and C. F. Fontán, *J. Comput. Phys.* **76**, 192 (1988).
22. B. Fornberg and G. B. Whitham, *Phil. Trans. R. Soc. London A* **289**, 373 (1978).
23. J. A. C. Weideman and B. M. Herbst, *SIAM J. Numer. Anal.* **23**, 485 (1986).
24. G. Chanteur, *Phys. Scripta* **33**, 233 (1986).
25. S. A. Orzag, *Stud. Appl. Math.* **50** (4), 293 (1971).
26. H. Schamel and K. Elsässer, *J. Comput. Phys.* **22**, 501 (1976).
27. D. J. Kaup and A. Newell, *J. Math. Phys.* **19**, 798 (1978).
28. M. Ablowitz, D. Kaup, A. Newell, and H. Segur, *Stud. Appl. Math.* **53**, 255 (1974).
29. J. Wyller, T. Flå, and E. Mjølhus, *Phys. D* **50**, 405 (1989).
30. T. Flå, E. Mjølhus, and J. Wyller, *Phys. Scripta* **40**, 219 (1989).
31. T. Flå, *Phys. Scripta* **40**, 206 (1989).
32. T. Taha and M. Ablowitz, *J. Comput. Phys.* **55**, 192, 203, 231 (1984).